Building Simulation 2005

Ninth International IBPSA Conference
Montréal, Canada
August 15-18, 2005

ASSESSMENT OF IMPACT OF BUILDING ENVELOPE POROSITY ON ENERGY

Kai Qiu, Fariborz Haghighat
Department of Building, Civil and Environmental Engineering, Concordia University, Montreal, Canada, H3H 1G8

ABSTRACT

This paper presents a numerical model for the analysis of impact of building envelope porosity on energy. In the porous envelope, the infiltrating air entering a building can change in temperature, along the infiltration path due to heat exchange between the air itself and the porous insulation matrix; hence the envelope effectively behaves as a heat exchanger. The presented model is based on combined airflow and heat transfer through porous media. Microscopic energy equations are formulated for solid and gas phases separately. Overall macroscopic heat transfer modeling is derived using volume average method and is applied for varying infiltration paths and porosity. Modeling results indicate that heat exchange performance is mainly determined by airflow rate with secondary influence from the infiltration path. Comparatively, under the same inlet velocity, the influence of porosity variation is not significant.

INTRODUCTION

A building envelope isolates a controlled indoor environment from the outdoors. Traditionally it is designed airtight to minimize costs of conditioning air. However, completely sealed buildings may lead to occupant dissatisfaction due to the deterioration of indoor air quality and in some cases increase the risk of Sick Building Syndrome (SBS). Therefore, there is a motivation to have the building envelope dynamically change related with the exterior environment (Gratia and De Herde, 2004). This can be achieved through the use of high porosity material in the envelope design.

Along with the development of advanced building envelopes, problems appear in the process of determining the energy consumption by the convectional method. Corresponding with the traditional building envelope design, the envelope is modeled as a multilayer solid system, and only the conductive heat transfer is considered. However, advanced building envelope intensively integrates the airflow in it, thus includes internal convective heat transfer processes due to the interaction of infiltrating air and the envelope itself. Therefore, to predict the thermal performance of advanced building envelopes, comprehensive analysis is required to consider the influence of conduction, convection, and infiltration as well as building material properties.

Generally, the infiltration heat loss, which is mainly due to airflow through the envelope, is estimated by assuming that a parcel of outdoor air maintaining its properties upon entering the air conditioned room. However, before the infiltrating air enters the building, it can change temperature along the infiltration path due to heat exchange between the air itself and the envelope's porous insulation. Thus the traditional method overestimates the actual heat loss. This was experimentally demonstrated by Bhattacharyya and Claridge (1995). Corresponding with the experimental investigation, they developed a one dimensional air cavity model, to describe the heat exchange process between the air and other parts of the envelope. This model is referred as the heat exchanger model, and was further simplified by Barhoun and Guarracino (2004) to derive an analytical solution, based on the assumption that an air cavity exists in the middle of the wall, and the air moves from the bottom to the top of the wall.

Considering the influence of building materials, a more appropriate model is to consider the heat exchange between the infiltrating air and the solid matrix of the porous building material. Adopting a constant air velocity in the wall, Krarti (1994) presented an analytical model for 1-D airflow and heat transfer. It was shown that heating load in the coupled process of conduction-infiltration through the porous wall is less than the simple summation of that due to conduction and infiltration. A numerical simulation for the heat recovery in the building envelope has been carried out by Buchanan and Sherman (2000). Their model incorporates heat transfer and airflow in the room, as well as that in the porous building envelope. However, their model does not focus on the heat exchange between the gas phase and the solid matrix. Only the effective thermal conductivity, obtained by an average of thermal conductivity of solid matrix and air, is used to represent the influence of porous media on heat

transfer in the envelope. Besides, the effect of variation of porosity on the energy impact is not discussed.

Airflow and heat transfer in porous media has been a research topic for decades and its state-of-art has been summarized by Bear (1972), Kaviany (1999) and Hsu (2003). Alazmi and Vafai (2002) comparatively investigated the typical models reported in the literature, by classifying them into four categories: constant porosity, variable porosity, Non-Local Thermal Equilibrium (NLTE) and thermal dispersion. Concerning the different heat transfer process in solid and moving fluid, for porous media with fluid flow through it, energy equations need to be set up for each phase separately. However if Local Thermal Equilibrium (LTE) is valid, i.e., the local average temperature difference of solid and fluid phase can be ignored, then the heat transfer in the entire material can be represented by only a single equation. In this case, the closure conditions introduced by volume average should be considered in the macroscopic energy equation to fully reflect the heat transfer performance in the microscopic structure.

This paper will begin from the microscopic point of view and discuss the heat exchange between the solid matrix and the infiltrating air. Numerical approaches are used to solve the governing equations. Parameter study will be performed for several scenarios, and effect of heat exchange process on energy consumption will be analyzed to illustrate the influence of inlet air velocity, infiltration path length and porosity.

MODEL DESCRIPTION

Airflow model

Model in this paper is set up for the case that dry air transfers through porous media while neglecting the influence of moisture. Meanwhile, as envelope's width is much larger than its thickness, and there is no buoyancy effect in the direction along the width of the envelope, 2-D model is adopted. This two dimensional treatment has significant advantage of simplifying CFD programming and reducing computational time.

As typical indoor and outdoor pressure differences for residential buildings are within the range of 0.1Pa to 10Pa (Abadie et al, 2002), airflow in the envelope is slow or creeping flow, thus it can be described by Darcy's law as follows:

$$\frac{\Delta p}{\Delta x} = \frac{\mu}{K} u \qquad (1)$$

Where the permeability of the porous media relates with the porosity of it according to Carmen-Kozeny theory (Kaviany, 1995), i.e.:

$$K = \frac{\varepsilon^3 d_p^2}{180(1-\varepsilon)^2} \qquad (2)$$

Equation (1) is the empirical relation accounting the macroscopic flow situation. To model the detail flow condition in the porous media, the volume average method for an elementary representative volume (REV), which has a length scale much larger than the pore diameter and smaller than the global length of the problem in consideration, is generally employed. The macroscopic equation obtained by this method is suitable for application, while including the necessary situations of the pore-level fluid flow. Following this methodology, a well-known semiheuristic equation is derived by Vafai and Tien (1981), and is expressed as

$$\frac{\rho_0}{\varepsilon^2}\left(\varepsilon\frac{\partial \mathbf{u}}{\partial t} + \mathbf{u}\cdot\nabla\mathbf{u}\right) = -\nabla p - \frac{\mu}{K}\mathbf{u} - \rho\mathbf{g} \qquad (3)$$

This equation corresponds with the Navier-Stokes equation for the pure fluid flow and influences of viscosity, inertia and buoyancy are included in it. In the current study, for the buoyancy term, which comes from density variation, Boussinesq approximation is adopted

$$\rho = \rho_0[1-\beta(T-T_0)] \qquad (4)$$

Heat transfer model

As air infiltration velocity is low through the building envelope, local thermal equilibrium is valid. This has been numerically demonstrated by Buchanan and Sherman (2000). Heat transfer in the building envelope is described by one medium treatment. However, heat transfer mechanism in the solid matrix and moving air are different; hence governing equations are formulated for each phase from the microscopic perspective.

Energy transfers through the solid matrix by conduction, and the process can be modelled as follows:

$$\frac{\partial T_s}{\partial t} = \alpha_s \nabla^2 T_s \qquad (5)$$

While it is best to include conduction and convection in the heat transfer process for infiltrating air

$$\frac{\partial T_a}{\partial t} + (\nabla\cdot\mathbf{u}T)_a = \alpha_a(\nabla\cdot\nabla T)_a \qquad (6)$$

For the LTE condition, the boundary conditions at the interface between solid matrix and air in a REV are

$$\mathbf{n}_{fs}\cdot k_a\nabla T_a = \mathbf{n}_{fs}\cdot k_s\nabla T_s \qquad (7)$$

$$T_s = T_a \tag{8}$$

By using volume average method and considering the influence of solid-air interface, the overall governing energy equation suitable for product level application is derived as:

$$[\varepsilon(\rho C_p)_a + (1-\varepsilon)(\rho C_p)_s]\frac{\partial T}{\partial t} + (\rho C_p)_a \mathbf{u}\cdot\nabla T = [\varepsilon k_a + (1-\varepsilon)k_s]\nabla\cdot\nabla T + (\rho C_p)_a \nabla\cdot k_d \nabla T \tag{9}$$

In equation (9), k_d is the thermal dispersion coefficient which accounts for the effect of fluctuation of local velocity distribution of pore-level airflow. By comparing numerical simulation results with experimental data, Jiang et al (1999) demonstrated that the thermal dispersion plays an important role in forced and mixed convective heat transfer in porous media, and must be included in the mathematical model for the case of one medium treatment. Meanwhile, their discussion shows that the influence of thermal dispersion is obvious for the fluid phase being either gas (air) or liquid (water).

The relation obtained by Koch and Brady (1986) through experiment for fibrous material is used for the thermal dispersion coefficient k_d in this study. It has the following form

$$k_d = \frac{\lambda\sqrt{K}|\mathbf{u}|}{\ln(\frac{1}{1-\varepsilon})} \tag{10}$$

Where

$$\lambda_x = \frac{57\pi^3}{160} \qquad \lambda_y = \frac{3\pi^3}{320} \tag{11}$$

Boundary conditions

Convective boundary conditions are considered to represent the influence of boundary layer at both surfaces inside and outside the room. For interior surface, it is expressed as:

$$-k\frac{\partial T}{\partial x} = h_{in}(T_{bi} - T_{in}) \tag{12}$$

As per ASHRAE (1993), the convective heat transfer coefficient h_{in} is defined as:

$$h_{in} = 1.87(\Delta T)^{0.32} H^{0.05} \tag{13}$$

While at the outside side, influence of radiation is also included. The heat balance at the exterior surface is

$$-k\frac{\partial T}{\partial x} = \alpha_{sol} I_t + h_r(T_{air} - T_{bo}) + h_{out}(T_{air} - T_{bo}) \tag{14}$$

Where the radiative heat transfer coefficient h_r is:

$$h_r = \varepsilon_s \sigma_s (T_{air}^2 + T_{bo}^2)(T_{air} + T_{bo}) \tag{15}$$

The convective heat transfer coefficient at exterior surface h_{out} is typically treated as a function of wind velocity. However, according to the data measured by Jayamaha et al (1996), it is approximately 6-10 W/m^{2}K. Thus a constant value of 10 W/m^{2}K was used in the simulation.

SOLUTION METHOD

The governing equations are solved by CFD approach. As it is a 2-D model and Boussinesq approximation is used to represent the variation of air density, the vorticity-stream function method is adopted. The stream function and vorticity are defined as follows

$$u = \frac{\partial \psi}{\partial y} \quad v = -\frac{\partial \psi}{\partial x} \tag{16}$$

$$\omega = \frac{\partial u}{\partial y} - \frac{\partial v}{\partial x} \tag{17}$$

While they are related by

$$\nabla^2 \psi = -\omega \tag{18}$$

Applying the definition of stream function and vorticity, the momentum equation (3) was transformed into the form containing the unknown variable of temperature T and vorticity ω. By assuming a temperature distribution, this equation can be solved to obtain values of ω. Followed by solving coupled equations (18), (16) and (9), a new temperature distribution can be acquired. Iteration repeats until obtaining the converged solution.

A uniform mesh is applied for each coordinate direction in the simulation and the equations are solved using an implicit finite difference method to assure the convergence.

In the solution process of each difference equation, Gauss-Seidel iteration accompanying with successive over-relaxation (SOR) is applied.

SIMULATION

The exterior building wall is taken as a typical example of building envelope and numerical simulations are performed for a wall 2.0m high and 0.2m thick. Four scenarios (illustrated in Fig 1) are employed in the current investigation to show the influence of infiltration path length. Configuration A

represents a straight through condition, while configurations B and C are low inlet-high outlet and high inlet-low outlet structure (Abadie et al, 2002). Configuration D is also a low inlet-high outlet situation while having a much longer air infiltration path length.

Meanwhile, simulation was performed for two porosity values of 0.8 and 0.9.

Indoor and the outdoor temperature are assumed to be 20 °C and 0°C, respectively. The simulation is performed under a range of inlet velocities, from 0.05m/s to 0.4 m/s.

The inlet velocity is closely related with wind speed, but is also influenced by other factors. For example, in case of a given wind speed, the porosity of the material will affect the inlet velocity value. To consider this effect, the pressure difference across the wall needs to be determined in advance according to the wind speed. Kinds of infiltration model have been developed on the relationship between pressure difference and wind velocity. However, they are mainly based on the experiments on leakage cracks and openings. Therefore, in the current simulation, the inlet velocity is directly treated as an input value, and the variation of inlet velocity under different porosity in case of a certain wind speed is not considered.

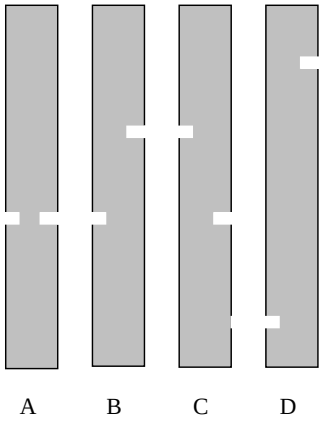

Figure 1: Scenarios in the simulation

In the simulation, converge criteria is set to 10^{-6}. To obtain the results that are not dependent on the grid, several types of mesh, i.e. 101×501, 101×1001, 151×1501, were tested. According to the test result, a 101×1001 mesh is fine enough to get the grid-independent solution and was selected for the simulation for all cases in the current study.

RESULTS AND DISCUSSION

By solving the developed model using the CFD method, temperature distribution in the wall can be obtained. Based on this, energy consumption under each case can be determined.

Temperature distribution

The simulation results first show that impacted by air infiltration, the temperature profile at inlet and outlet vicinity is quite different from that in the case of pure conduction. However, at most locations of the wall, heat transfer is dominated by conduction, if air is only allowed to enter the wall through a few minuscule cracks. Thus the entire wall can be divided into an area affected by air infiltration and one not affected. In the air infiltration affected area, heat exchange occurs as a result of forced convection. While other sections of the wall can still be modeled by conduction. According to this, it is possible to solve the problem analytically.

Another concern on the temperature distribution is the interior surface temperature. Figure 2 illustrates the change of average interior surface temperature with inlet velocity, under different air inlet and outlet configurations. From this, it can be seen that for straight through structure (configuration A), the average interior surface temperature is the highest. While for the configuration D, which the air enters and exits the wall at the position near the bottom and top separately, the average interior temperature is the lowest. The reason is that straight through configuration has the shortest air infiltration path, thus heat exchange in the wall is the least. As the air infiltration path becomes longer, more heat exchange occurs and this will result in the decrease of temperature in the area where air passes through. However, the result that the average interior surface temperature decreases under a longer infiltration path does not necessarily mean that this kind of configuration will have more obvious influence on the occupants' thermal comfort. In fact, in the case of high inlet-low outlet or low inlet-high outlet, though the average temperature is lower, the local temperature at the position of air entering the room is higher than that it is in the case of straight through configuration.

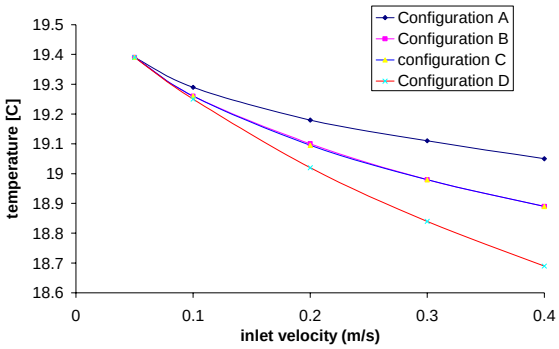

Fig 2: Average interior surface temperature change with inlet air velocity

Energy consumption

Figure 3 shows the result of heat flux at interior surface, which represents the energy consumption of each wall configuration. It can be seen that the potential for heat recovery is preferrable for configuration D.

Figure 4 indicates the relationship of total energy reduction with inlet air velocity under the four wall configurations. The impact of air infiltration can be seen: the total energy deduction reaches maximum value at an appropriate inlet velocity value. At low velocity, though heat exchange efficiency is high, as will be discussed later, the amount of total heat reduction is low due to the absolute low value of the infiltration heat loss calculated by conventional approach. The curves in this figure also demonstrate that potential of energy reduction is the lowest for the configuration A. Thus from the point of view of thermal performance, the air needs to be driven through the wall with an appropriate rate, along a path as long as possible, so that more heat exchange can occur before air enters the room.

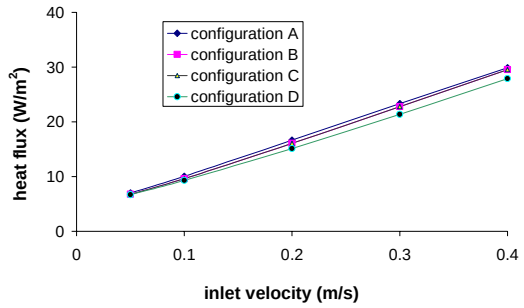

Fig 3: Relation of heat flux with inlet velocity

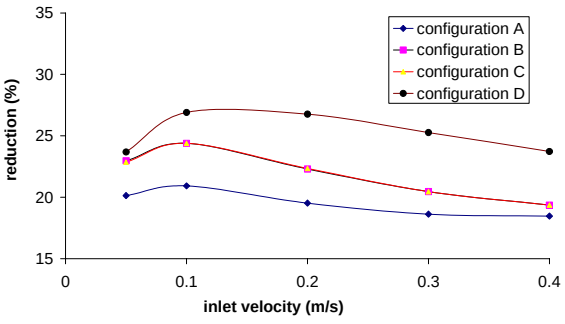

Fig 4: Change of the total heat reduction with inlet velocity

The Infiltration Heat Exchange Efficiency (IHEE) is defined to reflect the deviation of actual infiltration heat loss through the building envelope from the estimats obtained by the conventional approach by Claridge and Bhattacharyya (1995):

$$Q_{\inf} = (1-\eta)\dot{m}C_{pa}\Delta T \qquad (19)$$

Where ΔT is the indoor and outdoor temperature gradient. The coefficient η can be regarded as the scale of heat exchange performance in the building envelope.

Based on the temperature profile in the wall acquired by numerical simulation, IHEE η is calculated follows the approach presented by Buchanan and Sherman (2000), expressed as

$$\eta = 1 - \frac{Q - Q_0}{\dot{m}C_{pa}\Delta T} \qquad (20)$$

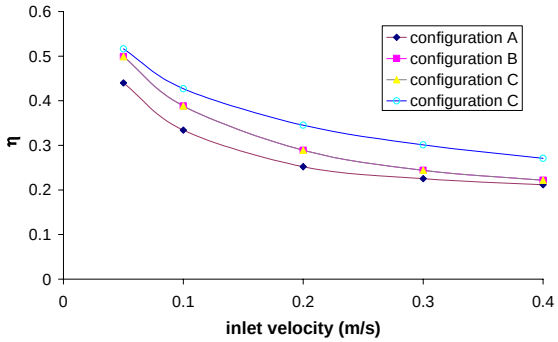

Fig 5: Relation of IHEE with inlet velocity under different configurations

Figure 5 shows the relationship of IHEE and the inlet velocity under different wall configurations, at a 0.9 porosity. It can seen that IHEE is high when the infiltration rate is low and it decreases with the increase of infiltration rate. At a very low infiltration rate, when the infiltrating air enters the building, it is almost warmed to the room temperature, due to the heat exchange phenomenon in the exterior wall. The temperature distribution inside the wall is almost the same as that without infiltration and little energy is required for the heat exchange process. As infiltration rate increases, though the infiltrating air can be warmed, the temperature difference between indoor air and incoming infiltrating air increases, and much energy is required for the heat exchange process, hence the IHEE decreases. Meanwhile, from the figure, it can be found that the infiltration path length is also an important factor for the heat exchange performance in the exterior wall. Comparatively, the configuration A has the least IHEE value at each inlet velocity, because its infiltration path is the shortest. However, under configuration D, the influence is more significant. Besides, the results in this figure as well as those in figures 3 and 4 illustrate that there is little difference

by adopting low inlet-high outlet or high inlet-low outlet structure for the reseach topic, as the curves of results for configuration B and configuration C are almost overlapped.

Figure 6 illustrates the change of IHEE with inlet velocity for the straight through wall (Case A) with a porosity of 0.9 and 0.8, respectively. It is shown that with an increase in the porosity, the heat exchange performance decreases. This demonstrates again the heat exchange occurs between solid matrix of the wall and the infiltrating air. The figure also shows that the difference of IHEE under two different porosity becomes smaller when air velocity increases. Of course, as it is pointed out before, the inlet velocity here is not directly determined by the windspeed. In real life, under a certain windspeed, the airflow rate under a lower porosity might be much smaller than it is under a higher porosity, thus IHEE under a lower posorisy could be obviously higher. However, even IHEE is higher in this case, the total heat loss reduction is smaller because of the greatly reduced airfow rate. On the other hand, though infiltration heat loss is lower when a low porosity material is used, the conduction heat loss increases because the thermal conductivity of solid matrix is greater than that of the air.

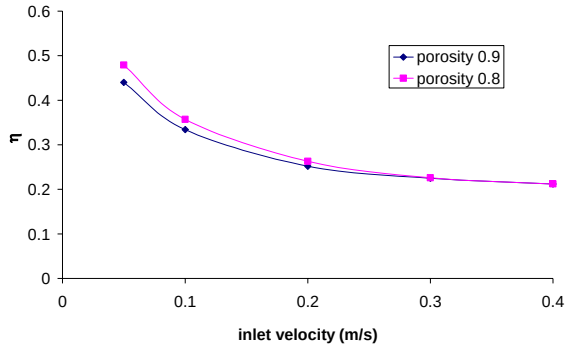

Fig 6: Relation of IHEE with inlet velocity under different porosity of the material

The above results are based on steady state simulation, corresponding with the traditional approach for the estimation of heat loss through the building envelope. In the current CFD simulation, a very small time step in the magnitude of second is used. Thus the hourly changed environment temperature will have little influence to the simulation result. However, as the incoming air exchanges heat with the solid matrix upon its entering the wall, dynamic effect is also important. As a matter of fact, at this stage, when air enters the room, its temperature is higher than that its reaching the steady state, hence the heat exchange efficiency will be higher. Research on transient property of heat exchange process in the porous media are among future tasks related to the topic of this paper.

CONCLUSION

Starting from the microscopic perspective, this paper investigates the heat exchange in porous building envelope and its impact on the energy consumption of buildings. Results by performing the numerical simulation for several air inlet-outlet configurations show that this phenomenon needs to be taken into account in order to precisely estimate the heat loss through the building envelope.

In each case under consideration, IHEE decreases when inlet air velocity increases, and total energy deduction reaches maximum at an appropriate inlet air velocity value, meaning that infiltration rate is the first important factor for the heat exchange performance in the building envelope.

Meanwhile, though it mainly occurs near air inlet and outlet position, heat exchange process between infiltrating air and solid matrix exists along the infiltration path. Thus IHEE is higher for the scenario having a longer infiltration path length.

The result which obviously demonstrates the heat exchange between infiltrating air and solid matrix is the relationship of IHEE and the porosity of the material. At the condition of lower porosity, more solid phase takes part in the heat exchange, thus IHEE is higher. However, the investigation also shows that under the same inlet velocity, the variation of porosity does not have an significant effect on the heat exchange performance of the building envelope, especially in high velocity range.

REFERENCES

Abadie, M. O., Finlayson, E. U., Gadgil, A J. 2002. Infiltration heat recovery in building walls: computational fluid dynamics investigations results, Lawrence Berkeley Laboratory, LBNL-51324.

Alazmi, B., Vafai, K. 2000. Analysis of variants within the porous media transport models. Transactions ASME, Journal of Heat Transfer, v122, n2, p303-326.

ASHRAE. 1993. Handbook of Fundamentals, American Society of Heating, Refrigerating and Air Conditioning Engineering.

Barhoun, H., Guarracino, G. 2004. Evaluating the energy impact of air infiltration through walls with a coupled heat and mass transfer method, Proceedings of CIB conference, Toronto Canada.

Bear, J. 1972. Dynamics of fluids in porous media. New York: Ameircan Elsevier Pub. Co.

Bhattacharyya, S., Claridge, D. E. 1995. Energy impact of air leakage through insulated wall, Journal of Solar Engineering, v117, n3, p167-172.

Buchanan, C. R., Sherman, M. H. 2000. A mathematical model for infiltration heat recovery, Lawrence Berkeley Laboratory, LBL-44294.

Gratia, E., De Harde, A. 2004. Natural cooling strategies efficiency in an office building with a double-skin façade, Energy and Buildings, v36, n11, p1139-1152.

Hsu, C-T. 2003. Heat and mass transport in porous media, Environmental Fluid Mechanics: Theories and Applications, p257-295.

Jayamaha, S. E. G., Wijeysundra, N. E., Chou, S. K. 1996. Measurement of the heat transfer coefficient for walls, Building and Environment, v31, n5, p399-407.

Jiang, P. X., Ren, Z. P., Wang, B. W. 1999. Numerical simulation of forced convection heat transfer in porous plate channels using thermal equilibrium and nonthermal equilibrium models, Numerical Heat Transfer, Part A: Applications. v35, n1, p99-113.

Kaviany, M. 1995. Principles of heat transfer in porous media, Second Edition, New York: Springer-Verlag.

Koch, D. L., Brady, J. F. 1986. Effective diffusivity of fibrous media, AIChE Journal, v32, n4, p575-591.

Krarti, M. 1994. Effect of airflow on heat transfer in walls. Journal of Solar Energy, v116, n1, p35-42.

Vafai, K., Tien, C. L. 1981. Boundary and initial on flow and heat transfer in porous media, International Journal of Heat and Mass Transfer, v24, p195-203.

NOMENCLATURE

C_{pa} Heat capacity of air (J/kg K)

C_{ps} Heat capacity of solid matrix (J/kg K)

d_p Pore diameter of the porous media (m)

h_{in} Convective heat transfer coefficient at interior surface (W/m^2K)

h_{out} Convective heat transfer coefficient at exteriot surface (W/m^2K)

h_r Radiative heat transfer coefficient at interior surface (W/m^2K)

H Height of the envelope (m)

I_t The solar radiation flux normal to the surface (W/m^2)

k Effective thermal conductivity of the envelope (W/m K)

k_a Thermal conductivity of air (W/m K)

k_d Thermal dispersion conductivity (W/m K)

k_s Thermal conductivity of solid matrix (W/m K)

K Permeability of the porous medium (m^2)

$\dot{m}$ Infiltration mass flow rate (kg/s)

$\mathbf{n}_{fs}$ Normal unit vector at solid-fluid interface (-)

p Pressure (Pa)

Q Heat loss through building envelope (W)

Q_{inf} Infiltration heat loss (W)

Q_0 Conduction heat loss (W)

t Time (s)

T Temperature (K)

T_0 Reference temperature of air of 273K (K)

T_a Temperature of air (K)

T_{air} Outdoor air temperature (K)

T_{bi} Boundary temperature at indoor side (K)

T_{bo} Boundary temperature at outdoor side (K)

T_{in} Indoor air temperature (K)

T_s Temperature of solid phase (K)

$\mathbf{u}$ Velocity (m/s)

x, y, Cartesian coordinates

α_a Thermal diffusivity of air (m^2/s)

α_{sol} The surface solar-absorption coefficient

α_s Thermal diffusivity of solid matrix (m^2/s)

β Expansion coefficient (1/K)

ε Porosity of the porous media

ε_s The surface emissivity

η Infiltraion heat exchange efficiency IHEE

λ_x, λ_y Nondimensional coefficient

μ Dynamic viscosity of the air (kg/m s)

ρ_0 Reference density of the air at 273K (kg/m^3)

ρ_a Density of the air (kg/m^3)

ρ_s Density of the solid matrix (kg/m^3)

σ_s The Stephan-Boltzman constant 5.67×10^{-8}